Journal of the Nigerian Association of Mathematical Physics
Volume 30, (*May, 2015*), pp117 – 130

Hollow Anode Cascading Plasma Focus

M. A. Alabraba

Department of Physics, Rivers State University of Science and Technology, Port Harcourt. Nigeria.

Abstract

Using the 3-phase model for each focus event, the 9-phase, two solid disc auxiliary anode cascading plasma focus has been extended to include holes at the center of each cascade anode (hereafter referred to as hollow anode cascading focus) with a view of increasing the neutron yield with each focus event. Results show that the hollow anode cascading focus like the solid anode exhibits good focusing characteristics, i.e. significant current dip, large voltage spike and fast radial piston speed. Comparing the neutron yields using established empirical scaling laws, the results show equal yield in the first focus phase, while the yield in the second and third focus phases is 1.7% and 2.8% respectively, lower than the solid anode.

Keywords: Cascading focus, Auxiliary hollow anode, 3-phase model

Nomenclature

a anode radius and also the forward path of current
a_1 radius of first cascade anode
a_2 radius of second cascade anode
a_{11} radius of the hole in the first cascade anode
a_{22}radius of the hole in the second cascade anode
b cathode radius and also the return pathof current
z time varying axial position of current sheath
z_0 length of inner electrode
z_f pinch elongation length
L_p inductance of plasma
L_{pj} inductance of plasma in phase j μ_0 magnetic permeability
V_{pj} induced voltage across plasma in phase j α first scaling parameter in axial R_P resistance of plasma phase
i instantaneous current
i_0 capacitor peak current
r_s radius of shock front
r_p piston radius radial phase
C_0 capacitance of capacitor bank
t_a axial transit time radial phase
t_0 capacitor discharge time
m_k mass of plasma in phase k
F_k axial force of plasma in phase k.

Greek symbols

ρ_0 ambient mass density
γ specific heat ratio
β second scaling parameter in axial phase
α_1 first scaling parameter in
β_1 second scaling parameter in

1.0 Introduction

In addition to its wide variety of uses, the plasma focus may eventually serve as an alternative source of energy, X-ray or neut rons. Moo et al [1] used metal and deuterated targets placed at various axial distances from the end of the anode of a 3-KJ UN U/ICTP plasma focus [2]. The result of their neutron measurement showed that about 85% of the neutrons were due to deuter on beam-gas target mechanism.

Corresponding author: M. A. Alabraba, E-mail: izzymatt2010@yahoo.com, Tel.: +2348037629953

During the measurement they were careful not to place the target less than 2cm from the primary anode of radius 1cm, since c urrent and voltage measurements have revealed that targets placed beyond a distance greater than the anode diameter did not affect the focusing dynamics. Lee et al [3] demonstrated this effect of target on focus dynamics by obtaining shadowgraphs i n the presence of a flat disc target placed at varying distances from the anode. It was found that the dynamics was not disturb ed when the target was placed at a distance greater than the anode radius. Beyond the focus proper the current sheath moved a xially to the disc target, climbed over it and pinched or focused again as though the target had become a new anode, thereby r esulting in two cascading focus events.

Based on this Lee [4] set up a model for two solid disc to produce three cascading focus events with each focus event made u p of an axial run down phase (A), a radial collapse phase (R) and a radial extension expanded column phase (RA)resulting in nine phases altogether.

Operating the cascading focus in deuterium, a neutron pulse is expected with each focus and since 85% of the neutrons are pr oduced by deuteron beam-gas target mechanism, the solid disc target is expected to produce fewer neutrons in the second and third focus events. This is because the targets will block the deuterons beam on its way to the second and third focus.

In the present set-up, using the 3KJ UNU/ICTP PFF with two auxiliary anodes downstream of the main anode, a hole was ma de in the center of each cascade anode

(See Fig. 1.)with the expectation that the deuteron beam would pass through and produce higher neutrons when compared wit h the solid cascade anode.

2.0 Theoretical Formulation

The 9-phase, two hollow auxiliary anode cascading plasma focus has three axial phases (a, d and g) in Fig. The snowplow mo del coupled to a circuit equation is used for the gross dynamics of the current sheath in terms of speed and trajectory. In the r adial phases (b, e and h) in Fig.1, a circuit coupled slug model [5, 6] has been used. In the radial extension phases (c, f and i) i n Fig.1, shadow graphic results show that there is no visible plasma column, consequently the model adopted is one in which the current path linking the anode to the moving current sheath is large and flows uniformly in a column. This uniform colum n is seen to extend through the holes of the cascade anode as shown in phase 4 i.e. d through to phase 9 i.e. i in Fig.1. For thes e phases, a snowplow model coupled to a circuit equation is again used. Using the equivalent circuit of Fig.2as well as the mo dels mentioned above, the equations in the different phases are as follows:

Phase 1: AI

$$L_{p1} = \frac{«_0}{2®} z \ln c$$

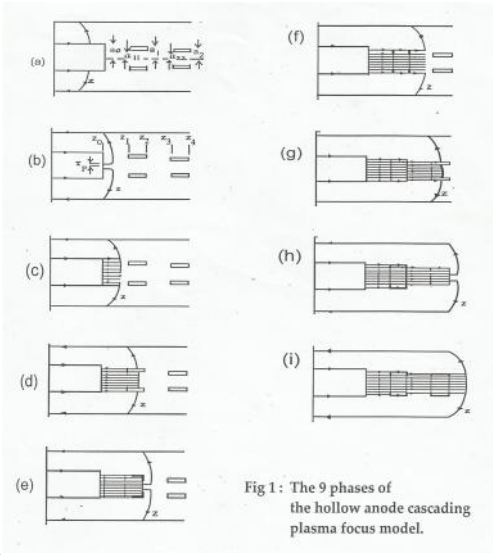

Fig 1 : The 9 phases of the hollow anode cascading plasma focus model.

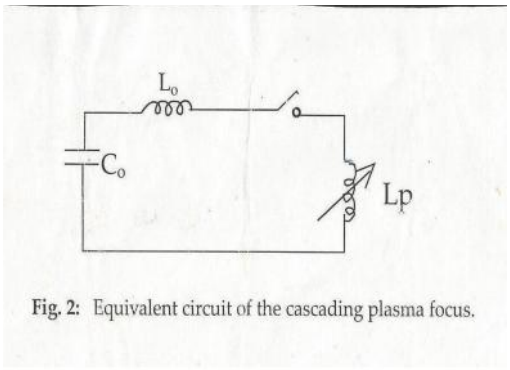

Fig. 2: Equivalent circuit of the cascading plasma focus.

The circuit equation is

$$\frac{d}{dt}\left[\left(L_0 + L_{p_1}\right)i\right] = V_0 - \frac{\int idt}{C_0} \qquad (1)$$

The snowplow model requires accumulation of mass [5,7] in the axial phases (AI,RAI, AII, RAII, AIII, RAIII) with correspo nding axial forces.

Mass loading $m_1 = ®°_0\left(c^2 - 1\right)a^2 z$

$$F_1 = \frac{\mu_0}{4\pi}(\ln c)i^2$$

Axial force

The equation of motion of the current sheath is

$$\frac{d}{dt}\left(m_1 \frac{dz}{dt}\right) = F_1 \tag{2}$$

Also the induced voltage using a purely inductive model is

$$V_{p1} = \frac{d}{dt}\left(L_{p1} i\right) \tag{3}$$

Phase 2: RI

$$L_{p2} = \frac{\mu_0}{2\pi}\left[(\ln c) z_0 + \ln\left(\frac{b}{r_p}\right) z_f\right]$$

For the radial phases (RI, RII, RIII), the radial magnetic piston drives a radially imploding shock front at position r_s according to the equation

$$\frac{dr_s}{dt} = -\sqrt{\left[\frac{\mu_0}{\rho_0}(\gamma+1)\right]}\frac{i}{4\pi r_p} \tag{4}$$

Since the compression is open ended, the same pressure drives the radial as well as the axial shock and so the column elongation rate is proportional to the radial collapse rate according to the equation

$$\frac{dz_f}{dt} = -\left(\frac{2}{\gamma+1}\right)\frac{dr_s}{dt} \tag{5}$$

Also the adiabatic law is applied to the plasma slug layer to determine the piston position r_p which follows the equation

$$\frac{dr_p}{dt} = \frac{\frac{2}{\gamma+1}\frac{r_s}{r_p}\frac{dr_s}{dt} - \frac{r_p}{\gamma i}\left(1-\frac{r_s^2}{r_p^2}\right)\frac{di}{dt} - \frac{1}{\gamma+1}\left(1-\frac{r_s^2}{r_p^2}\right)\frac{dz_f}{dt}\frac{r_p}{z_f}}{\frac{\gamma-1}{\gamma}+\frac{1}{\gamma}\frac{r_s^2}{r_p^2}} \tag{6}$$

The circuit equation is

$$\frac{d}{dt}\left[\left(L_0 + L_{p2}\right)i\right] = V_0 - \frac{\int i dt}{C_0} \tag{7}$$

The induced voltage is

$$V_{p2} = \frac{d}{dt}\left(L_{p2} i\right) \tag{8}$$

In this phase $z_f = z - z_0$

Phase 3: RAI

$$L_{p3} = \frac{\mu_0}{2\pi}\left[\ln c\left(z_0 + z_f\right) + \frac{z_f}{2}\right]$$

Here the current shrinks to a uniform current bunch of radius ‘a’ and the inductance contribution due to this bunch is $\frac{\mu_0}{2\pi}\frac{z_f}{2}$ (See Fig.1c). The circuit equation is

$$\frac{d}{dt}\left[\left(L_0 + L_{p3}\right)i\right] = V_0 - \frac{\int i dt}{C_0} \tag{9}$$

Mass loading $m_3 = \pi\rho_0 a^2\left[\left(c^2-1\right)z_0 + c^2 z_f\right]$

Since this phase completes the first focus event, the force will be

$F_3 = F_1 +$ force in the column

$F_3 = \frac{«_0}{4®}\left[\ln c + \frac{1}{4}\right]i^2$

i.e.

$\frac{«_0}{4®}\frac{i^2}{4}$ is the axial force contribution due to the column.

The equation of motion of the current sheath is

$$\frac{d}{dt}\left(m_3\frac{dz}{dt}\right) = F_3 \tag{10}$$

and the induced voltage is

$$V_{p3} = \frac{d}{dt}\left(L_{p3}i\right) \tag{11}$$

Phase 4 : AII

$$L_{p4} = \frac{«_0}{2®}\left[(\ln c)z_0 + \ln c_1(z - z_0) + \frac{1}{2}(z_1 - z_0) + \frac{1}{2}(z - z_1)d_{11}{}^2\right]$$

In this phase the bunch further shrinks to the radius $'a_1'$ to form a thin current sheath which is the beginning of the second fo cus event.

$\frac{«_0}{2®}\ln c_1(z - z_0)$ is the inductance contribution due to the space outside the bunch between z and z_0.

$\frac{«_0}{2®}\frac{(z_1 - z_0)}{2}$ is the inductance contribution due to the bunch between z_1 and z_0

$\frac{«_0}{2®}\frac{(z - z_1)}{2}d_{11}{}^2$ is the inductance contribution due to the bunch inside the hole.

The circuit equation is

$$\frac{d}{dt}\left[\left(L_0 + L_{p4}\right)i\right] = V_0 - \frac{\int i dt}{C_0} \tag{12}$$

Mass loading $m_4 = ®°_0 a^2\left\{\left(c^2 - 1\right)z_0 + \left(z - z_0\right)\left(c^2 + d_1{}^2\left(d_{11}{}^2 - 1\right)\right)\right\}$

The corresponding force is

$$F_4 = \frac{«_0}{4®}\left(\ln c_1 + \frac{d_{11}{}^4}{4}\right)i^2$$

$\frac{«_0}{4®}\frac{d_{11}{}^4}{4}i^2$ is the force contribution due to the column in the hole of cascade anode 1

The equation of motion of the current sheath is $\frac{d}{dt}\left(m_4\frac{dz}{dt}\right) = F_4$ (13)

while the induced voltage is

$$V_{p4} = \frac{d}{dt}\left(L_{p4}i\right) \tag{14}$$

Phase 5: RII

$$L_{p5} = \frac{«_0}{2®}\left\{(\ln c)z_0 + \ln c_1(z_2 - z_0) + \frac{(z_1 - z_0)}{2} + \ln\left(\frac{b}{r_p}\right)(z - z_2) + \frac{(z_2 - z_1)d_{11}{}^2}{2}\right\}$$

The equations for the shock front position eq. (4), the column elongation rate eq. (5) and the piston position eq. (6) remain the same while the circuit equation takes the form;

$$\frac{d}{dt}\left\{\left(L_0 + L_{p5}\right)i\right\} = V_0 - \frac{\int i dt}{C_0} \tag{15}$$

The induced voltage is

$$V_{p5} = \frac{d}{dt}\left(L_{p5} i\right) \tag{16}$$

Also in this phase $z_f = z - z_2$

Phase 6: RAII

$$L_{p6} = \frac{\mu_0}{2\pi}\left\{\left(\ln c\right)z_0 + \ln c_1\left(z - z_0\right) + \frac{\left(z_1 - z_0 + z - z_2\right)}{2} + \frac{\left(z_2 - z_1\right)d_{11}^{\ 2}}{2}\right\}$$

The circuit equation is

$$\frac{d}{dt}\left[\left(L_0 + L_{p6}\right)i\right] = V_0 - \frac{\int i dt}{C_0} \tag{17}$$

Mass loading is $m_6 = \pi r_0^{\ 2} a^2\left\{\left(c^2 - 1\right)z_0 + \left(z_2 - z_0\right)\left\{c^2 + d_1^{\ 2}\left(d_{11}^{\ 2} - 1\right)\right\} + c^2\left(z - z_2\right)\right\}$

The axial force is $F_6 = \frac{\mu_0}{4\pi}\left\{\ln c_1 + \frac{1}{4}\left(1 + d_{11}^{\ 4}\right)\right\} i^2$

$\frac{\mu_0}{4\pi}\frac{i^2}{4}$ is the force contribution due to the column beyond cascade anode 1.

$\frac{\mu_0}{4\pi} i^2 \frac{d_{11}^{\ 4}}{4}$ is the force contribution due to the column in the hole of cascade anode 1.

The equation of motion of the current sheath is

$$\frac{d}{dt}\left(m_6 \frac{dz}{dt}\right) = F_6 \tag{18}$$

while the induced voltage is

$$V_{p6} = \frac{d}{dt}\left(L_{p6} i\right) \tag{19}$$

Phase 7: AIII

$$L_{p7} = \frac{\mu_0}{2\pi}\left\{\left(\ln c\right)z_0 + \ln c_1\left(z_2 - z_0\right) + \ln c_2\left(z - z_2\right) + \frac{1}{2}\left(z_1 - z_0 + z_3 - z_2\right) + \frac{1}{2}\left(z_2 - z_1\right)d_{11}^{\ 2} + \frac{1}{2}\left(z - z_3\right)d_{22}^{\ 2}\right\}$$

Like phase 4, the bunch of current of radius 'a_1' shrinks further to radius 'a_2' to form a thin current sheath. This phase is the b eginning of the third focus event.

The circuit equation is

$$\frac{d}{dt}\left\{\left(L_0 + L_{p7}\right)i\right\} = V_0 - \frac{\int i dt}{C_0} \tag{20}$$

Mass loading m_7 is

$$m_7 = \pi r_0^{\ 2} a^2\left\{\left(c^2 - 1\right)z_0 + \left(z_2 - z_0\right)\left(c^2 + d_1^{\ 2}\left(d_{11}^{\ 2} - 1\right)\right) + \left(z - z_2\right)\left(c^2 + d_2^{\ 2}\left(d_{22}^{\ 2} - 1\right)\right)\right\}$$

$$F_7 = \frac{\mu_0}{4\pi}\left\{\ln c_2 + \frac{d_{22}^{\ 4}}{4}\right\} i^2$$

Axial force

The equation of motion can therefore be written as

$$\frac{d}{dt}\left(m_7\frac{dz}{dt}\right)=F_7 \tag{21}$$

Also the induced voltage follows the equation

$$V_{p7}=\frac{d}{dt}\left(L_{p7}i\right) \tag{22}$$

Phase 8: RIII

$$L_{p8}=\frac{\ll_0}{2\circledR}\left\{\begin{array}{l}(\ln c)z_0+\ln c_1(z_2-z_0)+\ln c_2(z_4-z_2)+\ln\left(\frac{b}{r_p}\right)(z-z_4)+\frac{1}{2}(z_1-z_0+z_3-z_2)+\\ +\frac{1}{2}(z_2-z_1)d_{11}{}^2+\frac{1}{2}(z_4-z_3)d_{22}{}^2\end{array}\right\}$$

The shock front position follows eq. (4) while the radial collapse rate follows eq. (5) and the piston position follows eq. (6). The circuit equation is

$$\frac{d}{dt}\left\{\left(L_0+L_{p8}\right)i\right\}=V_0-\frac{\int idt}{C_0} \tag{23}$$

and the induced voltage is

$$V_{p8}=\frac{d}{dt}\left(L_{p8}i\right) \tag{24}$$

In this phase $z_f=z-z_4$

Phase 9: RAIII

$$L_{p9}=\frac{\ll_0}{2\circledR}\left\{\begin{array}{l}(\ln c)z_0+\ln c_1(z_2-z_0)+\ln c_2(z-z_2)+\frac{1}{2}(z_1-z_0+z_3-z_2+z-z_4)+\frac{1}{2}(z_2-z_1)d_{11}{}^2+\\ +\frac{1}{2}(z_4-z_3)d_{22}{}^2\end{array}\right\}$$

The circuit equation is

$$\frac{d}{dt}\left\{\left(L_0+L_{p9}\right)i\right\}-V_0-\frac{\int idt}{C_0} \tag{25}$$

and the mass loading is

$$m_9=\circledR\,{}^\circ{}_0a^2\left\{\left(c^2-1\right)z_0+\left(z_2-z_0\right)\left(c^2+d_1{}^2\left(d_{11}{}^2-1\right)\right)+\left(z_4-z_2\right)\left(c^2+d_2{}^2\left(d_{22}{}^2-1\right)\right)+c^2\left(z-z_4\right)\right\}$$

while the axial force F_9 is

$$F_9=\frac{\ll_0}{4\circledR}\left\{\ln c_2+\frac{1}{4}\left(1+d_{22}{}^4\right)\right\}i^2$$

Therefore, the equation of motion is

$$\frac{d}{dt}\left(m_9\frac{dz}{dt}\right)=F_9 \tag{26}$$

and the induced voltage is

$$V_{p9}=\frac{d}{dt}\left(L_{p9}i\right) \tag{27}$$

3.0 Method of Solution

The equations in the different phases are non dimensionalized using the following parameters: $^2=\frac{t}{t_0},\S=\frac{i}{i_0},\neg=\frac{V_p}{V_0}$

For the axial phases, $, = \frac{z}{z_0}$ and for the radial phases, $k_s = \frac{r_s}{a}, k_p = \frac{r_p}{a}, , _f = \frac{z_f}{a}$

The resulting equations are:

Phase 1: AI

Equations (1), (2) and (3) become, respectively,

$$\frac{d\S}{d²} = \frac{1 - \int \S d² - \S \frac{d,}{d²}}{1 + \ ,} \tag{28}$$

$$\frac{d^2,}{d²^2} = \frac{\sim {}^2\S^2 - \left(\frac{d,}{d²}\right)^2}{,} \tag{29}$$

and $\neg_1 = \left\{, \frac{d\S}{d²} + \S \frac{d,}{d²}\right\}$ (30)

Equations (28) and (29) are integrated for the two time varying unknowns $,$ and $\S$ using the following procedure; With the starting values as

$${}^2{}_0 = 0 \ , \left(\int \S d²\right)_0 = 0 \ , \S_0 = 0 \ , \left(\frac{d\S}{d²}\right)_0 = 1 \ , \ , _0 = 0 \ , \left(\frac{d,}{d²}\right)_0 = 0 \ , \left(\frac{d^2,}{d²^2}\right)_0 = \sim\sqrt{\frac{2}{3}}$$

and a time increment $\Delta² = 0.001$,Euler's linear approximation method is employed to generate $\left(\int \S d²\right)_{n+1}$ and $\S_{n+1}$ from $\left(\frac{d\S}{d²}\right)_n$ using the equations; $\left(\int \S d²\right)_{n+1} = \left(\int \S d²\right)_n + \S_n \Delta² + \frac{1}{2}\left(\frac{d\S}{d²}\right)_n (\Delta²)^2$

$$\S_{n+1} = \S_n + \left(\frac{d\S}{d²}\right)\Delta²$$

and

Similarly $, _{n+1}$ and $\left(\frac{d,}{d²}\right)_{n+1}$ are generated from $\left(\frac{d^2,}{d²^2}\right)_n$ using the equations;

$$, _{n+1} = , _n + \left(\frac{d,}{d²}\right)_n \Delta² + \frac{1}{2}\left(\frac{d^2,}{d²^2}\right)_n (\Delta²)^2$$

$$\left(\frac{d,}{d²}\right)_{n+1} = \left(\frac{d,}{d²}\right)_n + \left(\frac{d^2,}{d²^2}\right)_n \Delta²$$

and

From the values of $\left(\int \S d²\right)_{n+1}$, $\S_{n+1}$, $, _{n+1}$ and $\left(\frac{d,}{d²}\right)_{n+1}$ together with equations (28) and (29) the next values of the derivatives $\left(\frac{d^2,}{d²^2}\right)_{n+1}$ and $\left(\frac{d\S}{d²}\right)_{n+1}$ can be generated.

This procedure continues until $,$ =1.

Phase 2: RI

Equations (4), (5), (6), (7) and (8) becom, respectively,

$$\frac{dk_s}{d²} = -\frac{\sim\sim_r \S}{k_p} \tag{31}$$

$$\frac{d, _f}{d²} = -\left(\frac{2}{¥ + 1}\right)\frac{dk_s}{d²} \tag{32}$$

$$\frac{dk_p}{d²} = \frac{\left(\frac{2}{¥+1}\right)\frac{k_s}{k_p}\frac{dk_s}{d²} - \frac{1}{¥}\frac{k_p}{§}\left(1-\frac{k_s^{\,2}}{k_p^{\,2}}\right)\frac{d§}{d²} - \left(\frac{1}{¥+1}\right)\frac{k_p}{,_f}\left(1-\frac{k_s^{\,2}}{k_p^{\,2}}\right)\frac{d,_f}{d²}}{\left(\frac{¥-1}{¥}\right)+\frac{1}{¥}\left(\frac{k_s^{\,2}}{k_p^{\,2}}\right)} \tag{33}$$

$$\frac{d§}{d²} = \frac{1-\int §d² + \ {}_f§\frac{,_f}{k_p}\frac{dk_p}{d²} + \ {}_f\left(\ln\frac{k_p}{c}\right)§\frac{d,_f}{d²}}{1+ \ - \ {}_f\left(\ln\frac{k_p}{c}\right),_f} \tag{34}$$

$$¬_2 = \left\{ \ - \ {}_f\left(\ln\frac{k_p}{c}\right),_f\right\}\frac{d§}{d²} - \ {}_f§\left\{\left(\ln\frac{k_p}{c}\right)\frac{d,_f}{d²} + \frac{,_f}{k_p}\frac{dk_p}{d²}\right\} \tag{35}$$

and

To start the integration, the following initializing values are used :

$k_s = 1$, $k_p = 1$, $,_f = 0.00001$ and the following final values of $²,\int §d²,§$ and $\frac{d§}{d²}$ of phase 1. The time increment $\Delta²$ for all the radial phases is taken as 0.00002. The integration is carried out using Eulers linear approximation for the four time varying unknowns $k_s,,,_f,k_p$ and § until $k_s = 0$

Phase 3: RAI

Equations (9), (10) and (11), respectively normalize to

$$\frac{d§}{d²} = \frac{1-\int §d² - \ §\frac{d,}{d²}L_2}{1+ \ + \ (, -1)L_2} \tag{36}$$

$$\frac{d^2,}{d²^{\,2}} = \frac{\sim {}^2§^2L_1 - h\left(\frac{d,}{d²}\right)}{1+h(, -1)} \tag{37}$$

$$¬_3 = \ \left\{\left(1+\frac{1}{2\ln c}\right)(, -1)+1\right\}\frac{d§}{d²} + \ \left(1+\frac{1}{2\ln c}\right)§\frac{d,}{d²} \tag{38}$$

The integration in this phase uses as initializing values the following final values of phase2 : $²,\int §d²,§$ and $, = 1+\frac{,_f}{F}$ (where we have re-normalized $,_f$ to z_0).

Also since the dynamics in this phase is similar to phase 1, initial value of $\frac{d,}{d²}$ is taken as its final value in phase 1. The int egration proceeds using Euler's linear approximation for $,$ and § until $, = ,_1 = \frac{z_1}{z_0}$.

Phase 4 : AII

The normalized forms of equations (12), (13) and (14) are, respectively,

$$\frac{d§}{d²} = \frac{1-\int §d² - \ §\frac{d,}{d²}L_{44}}{1+ \ + \ L_3(, -1)+\frac{}{2\ln c}(,_1-1)+\frac{d_{11}^{\ 2}}{2\ln c}(, -,_1)} \tag{39}$$

$$\frac{d^2,}{d²^{\,2}} = \frac{\sim {}^2§^2L_{33} - h_{11}\left(\frac{d,}{d²}\right)^2}{1+h_{11}(, -1)} \tag{40}$$

$$\neg_4 = \left\{\left(1+L_3(,-1)+\frac{1}{2\ln c}(,_1-1)+\frac{d_{11}{}^2}{2\ln c}(,-,_1)\right)\frac{d\S}{d^2}+L_{44}\S\frac{d,}{d^2}\right\} \tag{41}$$

The initializing values for this phase are the following final values of phase 3; i.e. $^2, \int \S d^2, , , \frac{d,}{d^2}$. The integration proceed s using Euler's linear method for , and $\S$ until $, = ,_2 = \frac{z_2}{z_0}$.

Phase 5 : RII

The equation for the shock front position remains as eq. (31). Also the column elongation rate remains as eq. (32) while the p iston position remains as eq.(33).

Equations (15) and (16) normalize, respectively, to

$$\frac{d\S}{d^2} = \frac{1-\int \S d^2 + \frac{{}_f\S,_f}{k_p}\frac{dk_p}{d^2} + {}_f\ln\left(\frac{k_p}{c}\right)\S\frac{d,_f}{d^2}}{1+ - {}_f\ln\left(\frac{k_p}{c}\right),_f + L_3(,_2-1)+\frac{}{2\ln c}(,_1-1)+\frac{d_{11}{}^2}{2\ln c}(,_2-,_1)} \tag{42}$$

$$\neg_5 = \left\{\begin{array}{l}\left(1+L_3(,_2-1)+\frac{1}{2\ln c}(,_1-1)\right)- {}_f\left(,_f\ln\left(\frac{k_p}{c}\right)-\frac{Fd_{11}{}^2}{2}(,_2-,_1)\right)\frac{d\S}{d^2}- \\ - {}_f\S\left(\ln\left(\frac{k_p}{c}\right)\frac{d,_f}{d^2}+\frac{,_f}{k_p}\frac{dk_p}{d^2}\right)\end{array}\right\} \tag{43}$$

The starting values for integration in this phase are the following final values of phase 4

which are : $^2, \int \S d^2, \S$ and $\frac{d\S}{d^2}$. Additional initializing values are :$k_s = d_1$, $k_p = d_1$, $\zeta_f = 0.00001$. The integration proceeds using Euler's linear approximation for the four time- varying unknowns k_s , k_p , ζ_f and $\S$ until $k_s = 0$

Phase 6: RAII

Equations (17) , (18) and (19) become, respectively

$$\frac{d\S}{d^2} = \frac{1-\int \S d^2 - \S\frac{d,}{d^2}L_4}{1+ + L_3(,-1)+\frac{}{2\ln c}(,-,_2+,_1-1)+\frac{d_{11}{}^2}{2\ln c}(,_2-,_1)} \tag{44}$$

$$\frac{d^2,}{d^{2\,2}} = \frac{\sim {}^2\S^2 L_{55} - h\left(\frac{d,}{d^2}\right)^2}{1+h_{11}(,_2-1)+h(,-,_2)} \tag{45}$$

$$\neg_6 = \left\{1+L_3(,-1)+\frac{1}{2\ln c}(,-,_2+,_1-1)+\frac{d_{11}{}^2}{2\ln c}(,_2-,_1)\right\}\frac{d\S}{d^2}+$$

$$+ \S\left(L_3+\frac{1}{2\ln c}\right)\frac{d,}{d^2} \tag{46}$$

In this phase the following final values of phase 5 are used as starting values : $^2, \int \S d^2, \S$ and $, = ,_2 + \frac{,_f}{F}$. Also the starting velocity $\frac{d,}{d^2}$ is taken as the final $\frac{d,}{d^2}$ of phase 4.

$$, = ,_3 = \frac{z_3}{z_0}$$

The integration proceeds until

Phase 7: AIII

Equations (20), (21) and (22) normalize, respectively, to

$$\frac{d\S}{d²} = \frac{1-\int \S d² - \S \frac{d,}{d²} L_{67}}{\left\{ \begin{array}{l} 1+ \quad + L_3(,_2 -1) + \quad L_6(, - ,_2) + \frac{}{2\ln c}(,_1 -1+ ,_3 - ,_2) + \frac{d_{11}{}^2}{2\ln c}(,_2 - ,_1) + \\ + \frac{d_{22}{}^2}{2\ln c}(, - ,_3) \end{array} \right\}} \tag{47}$$

$$\frac{d^2,}{d²^2} = \frac{\sim {}^2\S^2 L_{66} - h_{22}\left(\frac{d,}{d²}\right)^2}{1+h_{11}(,_2 -1)+h_{22}(, - ,_2)} \tag{48}$$

$$\neg_7 = \left\{ \begin{array}{l} 1+L_3(,_2 -1)+L_6(, - ,_2)+\frac{1}{2\ln c}(,_1 -1+ ,_3 - ,_2)+\frac{d_{11}{}^2}{2\ln c}(,_2 - ,_1)+ \\ + \frac{d_{22}{}^2}{2\ln c}(, - ,_3) \end{array} \right\} \frac{d\S}{d²} +$$

$$+ \quad \S\left\{ L_6 + \frac{d_{22}{}^2}{2\ln c} \right\} \frac{d,}{d²} \tag{49}$$

The final values of phase 6 used as starting values are : ², $\int \S d²$, §, , and $\frac{d,}{d²}$.

Equations (47) and (48) are integrated for § and , using Euler's linear approximation until $, = ,_4 = \frac{z_4}{z_0}$

Phase 8: RIII

The same set of equations (31), (32) and (33) are used respectively for the shock front position, column elongation rate and th e piston position.

Also equations (23) and (24) normalize to;

$$\frac{d\S}{d²} = \frac{1-\int \S d² + \frac{{}^f\S,_f}{k_p}\frac{dk_p}{d²} + \quad {}_f \ln\left(\frac{k_p}{c}\right)\S\frac{d,_f}{d²}}{\left\{ \begin{array}{l} 1+ \quad + L_3(,_2 -1)+ \quad L_6(,_4 - ,_2) - \quad {}_f \ln\left(\frac{k_p}{c}\right),_f + \frac{}{2\ln c}(,_1 -1+ ,_3 - ,_2)+ \\ + \frac{d_{11}{}^2}{2\ln c}(,_2 - ,_1) + \frac{d_{22}{}^2}{2\ln c}(,_4 - ,_3) \end{array} \right\}} \tag{50}$$

$$\neg_8 = \left\{ \begin{array}{l} \left(\begin{array}{l} 1+L_3(,_2 -1)+L_6(,_4 - ,_2)+\frac{1}{2\ln c}(,_1 -1+ ,_3 - ,_2)+ \\ + \frac{d_{11}{}^2}{2\ln c}(,_2 - ,_1)+\frac{d_{22}{}^2}{2\ln c}(,_4 - ,_3) \end{array} \right) - \\ - \quad {}_{f,f} \ln\left(\frac{k_p}{c}\right) \end{array} \right\} \frac{d\S}{d²} -$$

$$- \quad {}_f\S\left\{ \ln\left(\frac{k_p}{c}\right)\frac{d,_f}{d²} + \frac{,_f}{k_p}\frac{dk_p}{d²} \right\} \tag{51}$$

Initialization for this phase uses the following values: $k_s = d_2$, $k_p = d_2$, $\zeta_f = 0.00001$ and the following final values of phase 7 : z , $\int \S d^2$, $\S$ and $\frac{d\S}{d^2}$.

The integration proceeds until $k_s = 0$.

Phase 9 : RAIII

Equations (25), (26) and (27) are normalized, respectively to give

$$\frac{d\S}{d^2} = \frac{1 - \int \S d^2 - \S L_8\left(\frac{d_,}{d^2}\right)}{\left\{\begin{array}{l} 1 + \quad + L_3(,_2 - 1) + \quad L_6(, \; - ,_2) + \frac{}{2\ln c}(, \; - ,_4 + ,_3 - ,_2 + ,_1 - 1) + \\ + \frac{d_{11}^{\;2}}{2\ln c}(,_2 - ,_1) + \frac{d_{22}^{\;2}}{2\ln c}(,_4 - ,_3) \end{array}\right\}} \tag{52}$$

$$\frac{d^2,}{d^{2\,2}} = \frac{\sim {}^2\S^2 L_{77} - h\left(\frac{d_,}{d^2}\right)^2}{1 + h_{11}(,_2 - 1) + h_{22}(,_4 - ,_2) + h(, \; - ,_4)} \tag{53}$$

$$\neg_9 = \left\{\begin{array}{l} 1 + L_3(,_2 - 1) + L_6(, \; - ,_2) + \frac{1}{2\ln c}(, \; - ,_4 + ,_3 - ,_2 + ,_1 - 1) + \\ + \frac{d_{11}^{\;2}}{2\ln c}(,_2 - ,_1) + \frac{d_{22}^{\;2}}{2\ln c}(,_4 - ,_3) \end{array}\right\}\frac{d\S}{d^2} +$$

$$+ \quad \S\left\{L_6 + \frac{1}{2\ln c}\right\}\frac{d_,}{d^2} \tag{54}$$

The following final values of phase 8 are employed as initializing values : z , $\int \S d^2$, $\S$ and $, = ,_4 + \frac{,_f}{F}$. Also the final velocity $\frac{d_,}{d^2}$ of phase 7 is used as starting velocity.

The integration continues until $, = ,_5 = \frac{z_5}{z_0}$.

$z_5 = z_4 + z_4 - z_3$

4.0 Results and Discussion

We present the result of calculation carried out for the 9-phase hollow anode cascading plasma focus. Whereas Lee's 9-phase solid anode cascading focus was designed with the following parameters: $\alpha = 1.7$, $\beta = 0.27$, $F = 12.63$, $c = 3.37$, $\gamma = 1.667$, $\zeta_1 = 1.083$, $\zeta_2 = 1.167$, $\zeta_3 = 1.25$, $\zeta_4 = 1.33$, $d_1 = 0.895$, $d_2 = 0.737$; the hollow anode cascading plasma focus has the additional parameters: $d_{11} = 0.765$, $d_{22} = 0.714$. One further parameter called the differential pressure factor which takes account of the particle density difference in the axial and radial phases has been introduced as $F_p = 0.32$. These parameters correspond to operation at $V_0 = 15$KV with $C_0 = 30\mu$F, $L_0 = 110$nH, $a = 0.95$cm, $b = 3.2$cm, $z_0 = 12$cm, $z_1 = 13$cm, $z_2 = 14$cm, $z_3 = 15$cm, $z_4 = 16$cm, $a_1 = 0.85$cm, $a_2 = 0.70$cm, $a_{11} = 0.65$cm, $a_{22} = 0.50$cm and a pressure of 1torr deuterium. The results are given in Figs.3 –5.

Fig.3a shows the current $(\S)$ and Fig 3b voltage $(\neg)$ waveforms. The current rises and peaks at 0.788 in phase 2 on z =1.353 (i.e. about z =0.018 after the end of phase 1). It then drops to 0.773 which is lower by 1.9% of the peak value This steep drop in current gives rise to an induced voltage which spikes up to ν=3.23 on z =1.378 corresponding to a piston speed of 3.12

$\frac{z_0}{t_0}$

(seeFig. 5a) on the scale of characteristic speed of . Hence like the solid anode, the hollow anode cascading focus exhibits good focusing characteristics viz significant current dip, large voltage spike and fast radial piston speed.

The behavior in phases 3 and 4 is similar to Lee's solid anode, with the tube voltage dropping to a value of 0.343 which is sli ghtly higher than the final value of 0.273 in phase 1. The current remains practically constant at 0.772 dropping slightly to 0. 766 in phase 4.

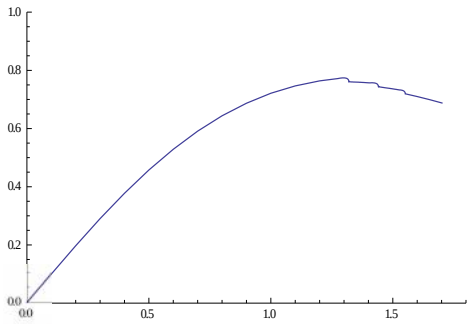

Fig 3a: Current waveform of the hollow anode focus with α=1.7 β=0.27, F=12.63, c=3.37
d_1=0.895, d_2=0.737, d_{11}=0.765, d_{22}=0.714, F_p=0.32

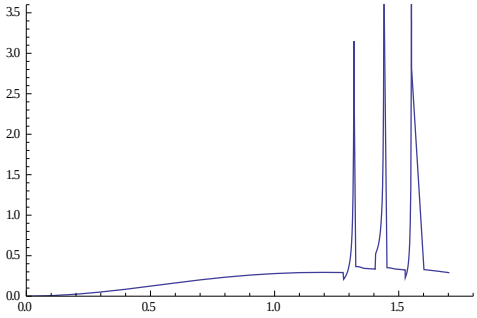

Fig 3b : Voltage waveform of the hollow anode focus with parameters same as in in Fig 3a

In phase 5 which is the radial phase of the second focus event, the current rises and peaks at 0.7663 on ^{2} =1.471. It then drop s to 0.7517 on ^{2} =1.504 which is again lower by 1.9% of the peak value. The voltage spikes up to 3.31 on ^{2} =1.503 correspo nding to a piston speed of 3.6 (see Fig. 5b). This radial collapse again exhibits all three characteristics of a good focus. Phases 6 and 7 have similar characteristics as the axial phases i.e. almost constant current of 0.749 and tube voltage of 0.329 which i s slightly higher than the final value of 0.313 in phase 4.

The third focus event occurs in phase 8 with a current dip again lower by 1.9% i.e. from 0.737 on ^{2} =1.592 to 0.723 on ^{2} =1. 617 and a voltage spike of peak value 3.67 on ^{2} =1.616 corresponding to a piston speed of 4.3 (see Fig. 5c). This focus event also has all three characteristic of a strong focus. Phase 9 completes the model with the plasma dynamics followed to the poi nt where voltage and current are brought down to values characteristic of the axial phase.

The scaling law for neutron yield (Y) with respect to maximum current (I_p) flowing in the pinch phase is $Y=DI_p^4$[8,9], D=1.7 $X10^{-13}A^{-4}$.

Fig.4a to 4c shows the pinch current for the solid and hollow cascade anode.

In phase 2 (see Fig.4a) the current is the same for both solid and hollow anodes indicating that the same number of neutrons will be produced. In phase 5 (see Fig.4b), the peak pinch current for the solid anode is 0.7694 while that of hollow anode is 0. 7662. Comparing the neutron yield gives Y_s=1.017Y_H thus the solid anode is expected to produce 1.7% more neutrons than th e hollow anode in phase 5. In phase 8 (see Fig.4c) the peak pinch current for the solid anode is 0.7422, while for the hollow a node, it is 0.7370. Comparing the neutron yield gives Y_s=1.028Y_H. This translates to the expectation that the solid anode will produce 2.8% more neutrons in phase 8 than the hollow anode.

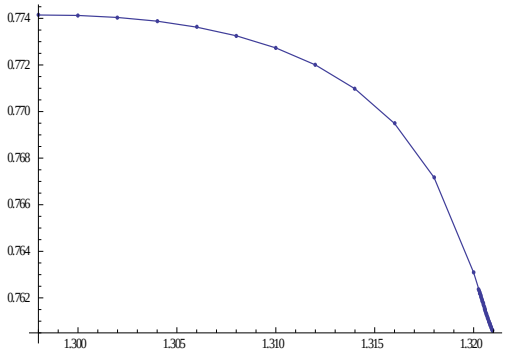

(a)

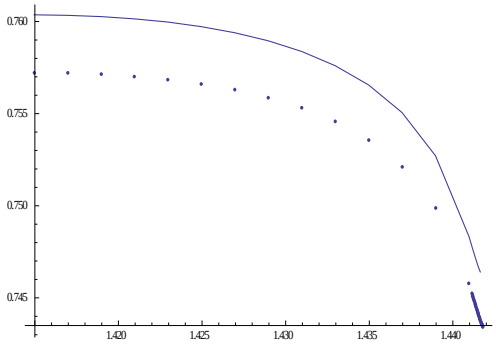

(b)

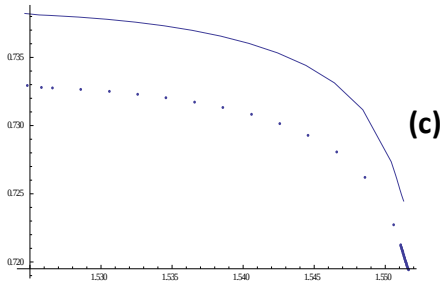

Fig. 4: Magnified version of current in the radial phases with parameters same as in Fig.3a
(a) phase2 (b) phase 5 (c) phase 8
solid line: current in solid anode focus
dotted line: current in hollow anode focus

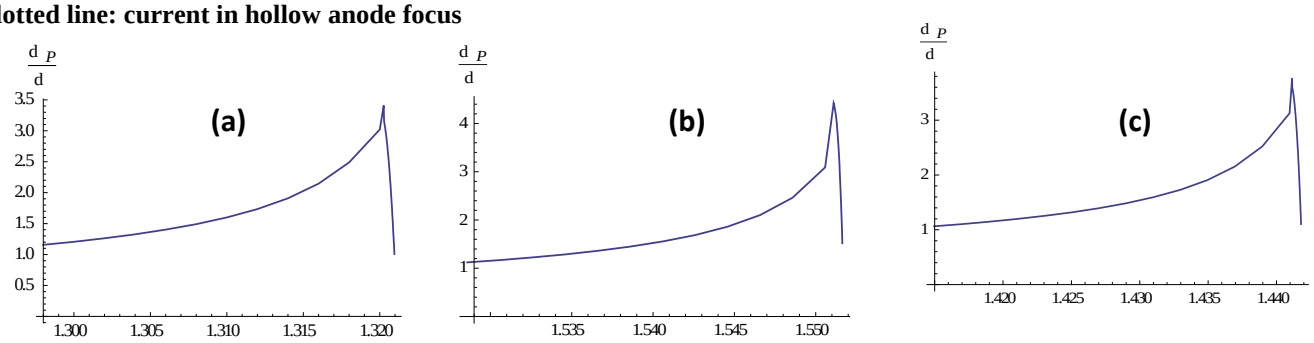

Fig 5: Radial piston speed of the hollow cascade anode
(a) In phase 2
(b) In phase 5
(c) In phase 8

5.0 Conclusion

The plasma focus event made up of three phases viz axial phase (A) followed by a radial phase (R) and a radial extension ex panded column phase (RA) has made it possible to compute all the main features observed experimentally. Byintroducing hol es atthe center of two auxiliary anodes to form a 9-phase hollow anode cascading plasma focus, we observe a cascade of focu s with a decreased neutron yield contrary to our expectation. A 3KJ UNU/ICTP plasma fusion facility has been used in the co mputation

Appendix A

The following constants have been used

$$c = \frac{b}{a}$$

$$t_0 = \sqrt{L_0 C_0}$$

$$\beta = \frac{Lp_j}{L_0}$$

$$\beta_1 = \frac{\beta}{lnc}$$

$$d_{22} = \frac{a_{22}}{a_2}$$

$$h_{11} = \frac{c^2 + d_1^2(d_{11}^2 - 1)}{c^2 - 1}$$

$$L_3 = \frac{lnc_1}{lnc}$$

$$L_6 = \frac{lnc_2}{lnc}$$

$$L_{33} = \frac{lnc_1 + \frac{d_{11}^4}{4}}{lnc}$$

$$L_{55} = \frac{lnc_1 + \frac{(1+d_{11}^4)}{4}}{lnc}$$

$$L_{67} = \frac{lnc_2 + \frac{d_{22}^2}{2}}{lnc}$$

$$t_a = \frac{\pi(c^2 - a^2)\rho_0}{i_0 I_0} \cdot \frac{z_0}{i_0}$$

$$\alpha = \frac{t_0}{t_a}$$

$$\alpha_1 = \frac{(\gamma+1)(c^2-1)^{\frac{1}{2}}}{lnc} \cdot \frac{F}{2}$$

$$d_{11} = \frac{a_{11}}{a_1}$$

$$h = \frac{c^2}{c^2 - 1}$$

$$h_{22} = \frac{c^2 + d_2^2(d_{22}^2 - 1)}{c^2 - 1}$$

$$L_4 = \frac{lnc_1 + \frac{1}{2}}{lnc}$$

$$L_8 = \frac{lnc_2 + \frac{1}{2}}{lnc}$$

$$L_{44} = \frac{lnc_1 + \frac{d_{11}^2}{2}}{lnc}$$

$$L_{66} = \frac{lnc_2 + \frac{d_{22}^4}{4}}{lnc}$$

$$L_{77} = \frac{lnc_2 + \frac{(1+d_{22}^4)}{4}}{lnc}$$

6.0 References

[1] S.P. Moo, C.K. Chakrabarty and S.Lee, An investigation of ion beam of a plasma focus using a metal obstacle and deuterated target, IEEE Trans. Plasma Sci. 19 (1991)515

[2] S.Lee, T.Y. Tou, S.P. Moo, M.A. Eissa, A.V. Gholap,K.H. Kwek, S. Mulyodrono, A.J. Smith, Suryada, W. Usada and M, Zakaullah, A simple facility for the teaching of plasma dynamics and plasma nuclear fusion, Amer. J. Physi cs 56, 1 (1988) 62-68

[3] S. Lee, M.A. Alabraba, A,V. Gholap, S. Kumar, K,H, Kwek, M. Nisar, R.S. Rawat and J. Sing, Effects of targets o n plasma focus dynamics, IEEE Trans. Plasma Sci. 18 6 (1990) 1028-1032.

[4] S. Lee, Asequential plasma focus, IEEE Trans. Plasma Sci.19 5 (1991) 912-918.

[5] S. Lee, Radiations in plasma,B.MacNamara, World Scient. Pub. Co. (1984) 967-977.

[6] D. Potter, The formation of high density Z-pinch, Nucl. Fusion 18, 6 (1978) 813-823.

[7] M. Rosenbluth and R. Garwin, Los Alamos Sci. Lab. Report,LA-1850 (1956).

[8] H. Schmidt, Proc. of II Latin Amer. Workshop on plasma physics and controlledthermonuclear fusion CIF series 12 (1987) 1-30

[9] M. Zakaullah, A parametric study of dense plasma focus, Ph.D thesis, Quaid-I-Azam Univ. Islamabad, Pakistan (1988).